

Im zweiten Teil des Buches wird die Optik und Anpassung der Kontaktlinsen behandelt. Auch hier wurde mit viel Fleiß alles zusammengetragen, dessen die Autoren habhaft werden konnten. Es fehlen jedoch auch hier die neuesten Entwicklungen auf diesem Gebiete, wie z. B. die Konoid-Kontaktlinsen, die vor zwei Jahren auch in Europa bekannt geworden ist und mit gutem Erfolg verwendet wird. Man vermißt bei der Darstellung der Fluoreszenzbilder Farbphotographien von echten Beispielen, die durch die Skizzen und Zeichnungen wohl kaum ersetzt werden können.

Es besteht ein echter Bedarf für ein Fachbuch für Augenoptiker, das sich mit Fragen der Brillenanpassung und Anpassung von Kontaktlinsen befaßt. Diese Lücke, die hier vorhanden ist, wird durch das vorliegende Werk jedoch nicht in zufriedenstellendem Maße geschlossen.

J. Reiner

### Handbuch der Physik Band XXV/2c: Licht und Materie 1c.

H. Haken, Laser Theory, Springer Verlag 1970, 320 Seiten, DM 120,-.

Der vorliegende neue Band des Handbuches der Physik beinhaltet ausschließlich den Beitrag von H. Haken. Seit 10 Jahren hat sich der Autor mit den theoretischen Grundlagen des Lasers beschäftigt und dazu eine Reihe originärer Beiträge geliefert. Unter Hinstellung experimentell-technischer Probleme oder gar von Anwendungsaspekten, wird die Funktion des Lasers in theoretischer Methodik auf fundamentalprozesse zurückgeführt, wobei die klassische Theorie elektromagnetischer Felder mit der Quantentheorie atomarer Systeme und statistischer Prozesse verbunden wird.

Diese theoretisch anspruchsvolle Behandlung erstreckt sich auf alle mit der Lasersaktion verbundenen Teilfragen, z. B. mit dem optischen Resonator, den Intensitätsverhältnissen, den Moden-Stabilitäten, dem Impulsbetrieb und den Kohärenzeigenschaften. Erfüllt werden sowohl der Gas- als auch der Festkörperlaser. In allen Fällen ist die Behandlung so allgemein, daß die Ergebnisse auch auf Lasers übertragen werden können. Eine Reihe der für das Verständnis des analogen Systeme z. B. Systeme mit großer Abweichung von thermischen Gleichgewicht, nicht lineare Systeme oder Phasenübergänge in Systemen angewendet werden. Den zuletzt genannten Gesichtspunkt hat der Autor, es sei erlaubt den Leser darauf hinzuweisen, im Hauptvortrag des Fachausschusses Halbleiterphysik 1970 in Pfrontenstadt (Festkörperprobleme X, Herausgeber O. Madelung, Vieweg-Verlag 1970) unter dem Thema „Laserslicht – ein neues Beispiel für eine Phasenumwandlung“ erweitert dargestellt.

Obwohl die Laserliteratur mit etwa 2000 Publikationen pro Jahr eine enorme Zuwachsrate besitzt, wird der vorliegende Handbuchband aufgrund seines fundamental-theoretischen Konzepts ein permanent wichtiges Hilfsmittel für den auf dem Laser-Gebiet forschend tätigen Physiker sein.

Ernst Rudolf Kießler

### Taugungen

3. Internationaler Kongreß für Stereologie in Bern (Schweiz) vom 26. bis 31. August 1971. Auskunft durch das Kongreß-Büro im Anatomischen Institut, Bühlstrasse 26, CH-3000 Bern.

„Einführung in die Farbmetrik“, Kurs gehalten von Prof. Dr. M. Richter, Berlin, am 16./17. November 1970 in der Technischen Akademie, 56 Wuppertal-Elberfeld, Hubertusallee 18. Auskunft durch die Akademie.

„Praktische Farbmessung“, Kurs bei der Bundesanstalt für Materialprüfung, I Berlin 45, Unter den Eichen 87, vom 3. bis 14. Mai 1971. Auskunft durch die Bundesanstalt.

# Optik

Zeitschrift für Licht- und Elektronenoptik

Fachorgan der Deutschen Gesellschaft für Elektronenmikroskopie und der Deutschen Gesellschaft für angewandte Optik

Begründet von Fritz Gässler und Norbert Günther · Herausgegeben von Erich Menzel

WISSENSCHAFTLICHE VERLAGSGESELLSCHAFT MBH · STUTTGART

BAND 32

HEFT 3

1970

## Beam Displacement at Total Reflection: II\*

### The Goos-Hänchen Effect, II\*

By Helmut K. V. Lotsch\*\*

Institut für Theoret. Elektrotechnik, TH Aachen, Germany

Received 1. April 1970

### Abstract

The paper is divided into four parts. Part I comprises the Introduction and the two chapters entitled "Reflection and Refraction of a Beam of Light" and "Total Reflection of an E-Polarized Beam". Part II treats the Goos-Hänchen effect in classical optics. The different descriptions are compared and their results are compared with Wolter's measurements. Part III deals with the Goos-Hänchen effect in other branches of physics such as acoustics, quantum mechanics, plasma physics and nonlinear optics. The Schoch effect is introduced; furthermore the total reflection of diverging and converging waves is investigated. The final Part IV is devoted to several applications of the Goos-Hänchen effect, including the case of absorbing media. In addition, it contains the Summary and Conclusion, and the extensive list of references.

### Inhalt

**Strahlversetzung bei der Totalreflexion.** Die vorliegende Arbeit ist in vier Teile unterteilt. Teil I umfaßt die Einleitung und die beiden Kapitel „Reflexion und Brechung eines Lichtstrahles“ und „Totalreflexion eines E-polarisierten Lichtstrahles“. Teil II behandelt den Goos-Hänchen-Effekt in der klassischen Optik. Die verschiedenen Beschreibungen werden besprochen, und ihre Ergebnisse mit den Messungen von Wolter verglichen. Teil III befaßt sich mit dem Goos-Hänchen-Effekt

\* Dissertation approved by the Faculty of Electrical Engineering at the Technical University of Aachen, translated into English.

\*\* Author's address: Aeronetics Division of North American Rockwell, Anaheim, California 92803.

in anderen Zweigen der Physik, nämlich der Akustik, der Quanten-Mechanik, der Plasma-Physik und der nichtlinearen Optik. Der Schock-Effekt wird eingeführt; ebenso wird die Totalreflexion divergierender und konvergierender Wellen untersucht. Der abschließende Teil IV ist einigen Anwendungen des *Goos-Hänchen*-Effektes, einschließlich dem Fall absorbierender Medien, gewidmet. Außerdem enthält er die Zusammenfassung und Schlußbetrachtung und das ausführliche Literaturverzeichnis.

### 3. The Goos-Hänchen Effect in Classical Optics

*Goos* and (*Lindberg*-)*Hänchen* [1] have experimentally demonstrated that, in the plane of incidence, the totally reflected, linearly polarized beam of light is displaced parallel to a ray which would be reflected geometrically at the interface. They concluded, as already suspected by *Newton* [2], that, even at total reflection, the incident beam penetrates into the optically less-dense medium and then re-emerges into the optically denser medium; in other words, that the beam is reflected by some virtual surface located at a small distance within the less-dense medium. This so-called *Goos-Hänchen* effect can be expressed equivalently either as a beam displacement  $D$ , as a depth of penetration  $Z$ , or as a shift of the reflection center  $X$ ; the notation is defined in Fig. 1. In the present paper emphasis is placed on the beam displacement for historical reasons;  $Z$  and  $X$  are easily obtained from the following relations

$$Z = D / (2 \sin \varphi) \quad (32a)$$

and

$$X = D / \cos \varphi. \quad (32b)$$

noting that  $D = D(\varphi)$  is a function of the angle of incidence  $\varphi$ .

Although the problem can be formulated rigorously, perhaps departing from the References 7 and 20, its analytical treatment is so involved that a simple solution has not been achieved to date. Therefore, in a manner similar to *v. Fragsstein* [12], we explain the *Goos-Hänchen* effect on the basis of the *Schäfer* and *Pichl* pictorial interpretation of the flow of light energy at total reflection, presented in the preceding section. The reflection seems to be slightly less than total in  $B'$  and slightly more than total in  $B_r$ , as indicated in Fig. 4. The line of gravity of the totally reflected beam, representing the displaced with respect to a geometrically reflected beam, representing the *Goos-Hänchen* effect. The beam displacement as well as the depth of penetration are treated in Section 3.1 for both polarizations. The respective expressions yield, in agreement with *Renard's* viewpoint [13], the physically meaningful result that the *Goos-Hänchen* effect vanishes in the limit of grazing incidence. These general expressions are rather involved. They can be simplified substantially if only angles close to the critical angle for total reflection are considered.

*Artmann* [15] and *Wolter* [16] developed theories for the *Goos-Hänchen* effect on the basis of physical optics, which are treated in Section 3.2. Their basic idea rests upon *Noether's* simple interpretation [8] of *Pichl's* cumbersome theory of total reflection [7], outlined in Section 1.0. Both investigated the total reflection of two plane waves propagating under a small angle with

respect to one another. *Artmann* assumed a superposition in-phase and considered the propagation of the resultant maximum. He showed that his results so deduced can also be obtained on the basis of a complete plane-wave expansion, but the derivation is much more involved. On the other hand, *Wolter* assumed a superposition out-of-phase and considered the propagation of the resultant minimum. This method of the minimum-ray definition [21] enables one to measure the beam displacement with high precision. In fact, *Wolter* demonstrated perfect agreement between theory and experiment for angles close to the critical angle for total reflection. It is, therefore, concluded that the *Artmann-Wolter* expressions for the *Goos-Hänchen* effect, although not quite satisfactory in the limit of grazing incidence, are simple and accurate enough to warrant their application in most practical cases.

*Wolter's* theory [16] provides the possibility of accounting for absorption. This feature is briefly indicated in Sections 3.2 and 3.3; but a detailed discussion is deferred to Section 6.2.

Section 3.3 is concerned with the narrow angle range about the critical angle for total reflection which has so far been excluded for reasons stated in Section 1.2. The two plane-wave components representing the incident beam are studied in the transition region from total to partial reflection on the basis of *Wolter's* extended theory [16]. The limiting case, when these components propagate in the same direction, was treated by *Artmann* [44]. He noted that, as an angle of incidence approaches the critical angle for total reflection, the intensity distribution of the beam is distorted and its reflection center shifts by a finite rather than an infinite amount.

Finally, it should be mentioned that an aperture, introduced in front of the interface to cut a beam from an incident plane wave, causes a small polarization-dependent beam displacement [45]. The displacement is parallel to the direction of propagation and results from the electromagnetic boundary conditions which must be satisfied at the edge of the aperture. In the classical experiment of *Goos* and *Hänchen* [1] this phenomenon is negligible since it arises only once, whereas the beam displacement at total reflection is magnified by the multiple reflections.

#### 3.1 General Description Based on the Flow of Light Energy

The *Goos-Hänchen* effect expressed by the beam displacement  $D$  can be written in the general form, [3]

$$D_{\perp, \parallel} = (\lambda/2\pi) \operatorname{Re} \{ (a_{\perp, \parallel} + r_{\perp, \parallel}) / iR_{\perp, \parallel} \}, \quad (33)$$

where  $\operatorname{Re} \{ \dots \}$  stands for "real part of  $\{ \dots \}$ ". On substituting the respective relations from (13) through (17) we obtain for the  $E$  polarization

$$D_{\perp} = \frac{\lambda}{\pi} \frac{\sin \varphi}{\sqrt{\sin^2 \varphi - \sin^2 \varphi_c}} P_{\perp}(\varphi), \quad (34)$$

with the shorthand

$$P_{\perp}(\varphi, \Phi) = \frac{1 - \sin^2 \varphi}{1 - \sin^2 \Phi}, \quad (35)$$

and for the H polarization

$$D_{\parallel} = \frac{\lambda}{\pi} \frac{\sin \varphi}{\sqrt{\sin^2 \varphi - \sin^2 \Phi}} P_{\parallel}(\varphi, \Phi) \quad (36)$$

with the shorthand

$$P_{\parallel}(\varphi, \Phi) = \frac{\sin^2 \Phi (\sin \varphi \cos^2 \Phi - \sin^2 \varphi + \sin^2 \Phi)}{\sin \varphi (\sin^4 \Phi \cos^2 \varphi + \sin^2 \varphi - \sin^2 \Phi)}, \quad (37)$$

where  $n$  has been replaced by  $\sin \Phi$  according to (18). The *Goos-Hänchen* effect is thus represented by a product of two functions. The first function is common to both  $D_{\perp}$  and  $D_{\parallel}$ , whereas the second depends upon the polarization. The singularity of the common function is immaterial since, as we recall from Section 1.2, the immediate neighborhood of  $\Phi$  must be excluded. This narrow angle range (say,  $\varphi - \Phi < 0.3^\circ$ ) will be considered separately in Section 3.3.

The expressions (34) and (36) are plotted in Fig. 5 for three different values of the parameter  $\Phi$ . We see that the beam displacement decreases, first rapidly and then slowly, as the  $\varphi$  exceeds  $\Phi$ . In agreement with *Renard's* viewpoint [13] the beam displacement vanishes in the limit of grazing inci-

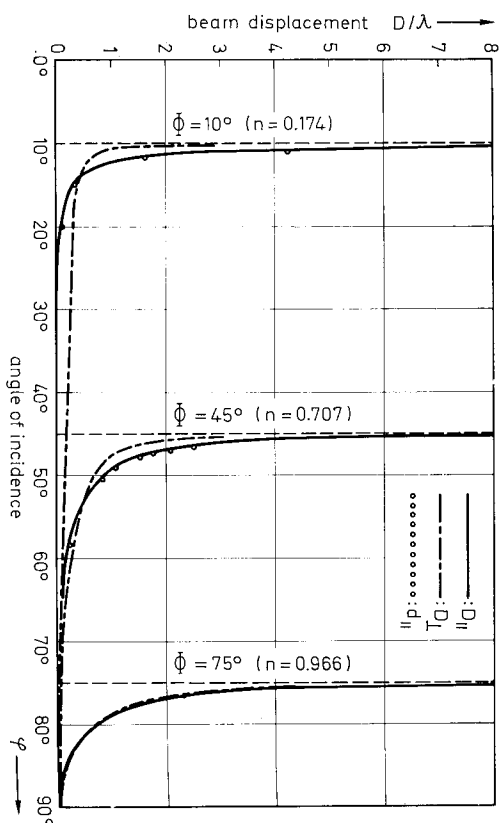


Fig. 5. The beam displacement  $D$  versus angle of incidence  $\varphi$  is displayed for three different values of the critical angle for total reflection  $\Phi$ . The open dots represent *Renard's* expression (40b) for H polarization. The wavelength  $\lambda$  is measured in the optically denser Medium.

dence, i. e., as  $\varphi \rightarrow \pi/2$ . Its dependence on the polarization is pronounced at small values of  $\Phi$  and diminishes as  $\Phi$  increases. In fact, the ratio  $(P_{\perp}/P_{\parallel})$  reduces to  $\sin^2 \Phi = n^2 \leq 1$  for  $\varphi \rightarrow \Phi$ , according to (35) and (37), and therefore approaches unity as  $\Phi \rightarrow \pi/2$ .

The totally reflected beam appears to have been reflected by a virtual surface at the distance  $Z$  within the less-dense medium; its center of reflection seems shifted by the amount  $X$  along the interface (see Fig. 1). Using (34) and (36) we obtain the depth of penetration  $Z$  from (32a)

$$\left. \begin{aligned} Z_{\perp} &= \frac{\lambda}{2\pi} \frac{1}{\sqrt{\sin^2 \varphi - \sin^2 \Phi}} P_{\perp}(\varphi, \Phi) \\ Z_{\parallel} &= \frac{\lambda}{2\pi} \frac{1}{\sqrt{\sin^2 \varphi - \sin^2 \Phi}} P_{\parallel}(\varphi, \Phi), \end{aligned} \right\} \quad (38)$$

and the shift of the reflection center from (32b)

$$\left. \begin{aligned} X_{\perp} &= \frac{\lambda}{\pi} \frac{\tan \varphi}{\sqrt{\sin^2 \varphi - \sin^2 \Phi}} P_{\perp}(\varphi, \Phi) \\ X_{\parallel} &= \frac{\lambda}{\pi} \frac{\tan \varphi}{\sqrt{\sin^2 \varphi - \sin^2 \Phi}} P_{\parallel}(\varphi, \Phi), \end{aligned} \right\} \quad (39)$$

where the polarization-dependent functions  $P(\varphi, \Phi)$  are defined by (35) and (37), respectively. It is interesting to note that  $X$  is undetermined in the limit of grazing incidence. This result appears quite reasonable since the beam would propagate along the interface without intersecting it.

The two expressions of (38) are plotted in Fig. 6 for three different values of the parameter  $\Phi$ . We see that, as in the case of the beam displacement, the depth of penetration is equally significant only in the vicinity of  $\Phi$ , recalling the exclusion of the immediate neighborhood of  $\Phi$ . The depth of penetration decreases, first rapidly and then slowly, as  $\varphi$  exceeds  $\Phi$ . In the limit of grazing incidence no light energy penetrates into the less-dense medium. The dependence on the polarization is the same as discussed above.

*Renard* [13] previously derived the beam displacement, likewise taking advantage of the conservation of energy. He noted that all energy propagating in the region M of the less-dense medium (see Fig. 4), described by  $S_{\alpha}^{\pm}$  of (30) with  $\alpha = 0$ , must return to the denser medium in the right border zone of the reflected beam. This flow of energy causes a displacement of the line of gravity of the totally reflected beam, amounting to, [13]

$$d_{\perp} = \frac{\lambda}{\pi} \frac{\sin \varphi}{\sqrt{\sin^2 \varphi - \sin^2 \Phi}} \left( \frac{\cos^2 \varphi}{\cos^2 \varphi + \sin^2 \varphi - \sin^2 \Phi} \right) \quad (40a)$$

for E polarization and to

$$d_{\parallel} = \frac{\lambda}{\pi} \frac{\sin \varphi}{\sqrt{\sin^2 \varphi - \sin^2 \Phi}} \left( \frac{\sin^2 \Phi \cos^2 \varphi}{\sin^4 \Phi \cos^2 \varphi + \sin^2 \varphi - \sin^2 \Phi} \right) \quad (40b)$$

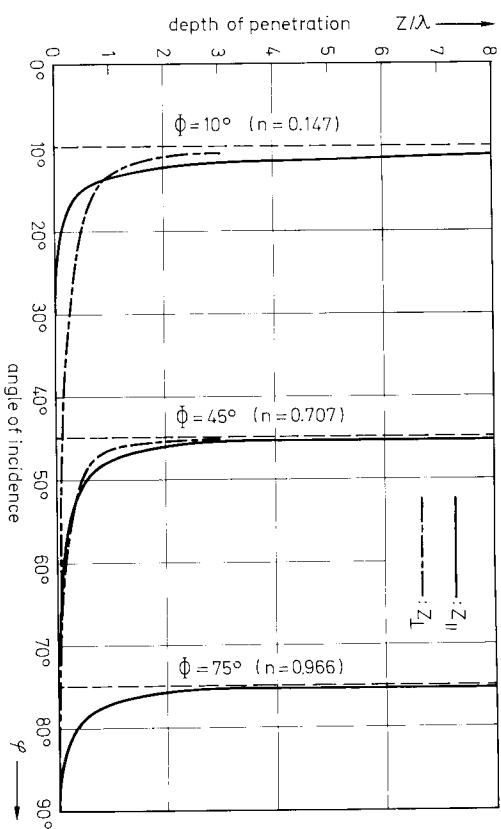


Fig. 6. The depth of penetration  $Z$  versus angle of incidence  $\varphi$  is displayed for three different values of the critical angle for total reflection  $\Phi$ . At  $\Phi = 75^\circ$  both polarizations exhibit essentially the same functional dependence. The wavelength  $\lambda$  is measured in the optically denser medium.

for H polarization. The former expression is obviously identical with (34), whereas the latter is slightly, but insignificantly different from (36). In fact, the numerical evaluation indicated by the open dots in Fig. 5 yields that the deviation is so small that both results, namely (36) and (40b), may be considered in full agreement for all practical purposes. The minute discrepancy originates from the fact that both derivations, strictly speaking, stem from approximate theories.

The polarization-dependent functions (35) and (37) can be simplified substantially if the angle of incidence  $\varphi$  is only slightly larger than the critical angle for total reflection  $\Phi$ . In this limit we have  $\sin \varphi \approx \sin \Phi = n_1$ , and the *Goos-Hänchen* effect can be represented approximately by the Artmann-V. Fragstein expressions ([12] and [15])

$$\left. \begin{aligned} D_{\perp} &\approx \frac{\lambda}{\pi} \frac{\sin \Phi}{|\sin^2 \varphi - \sin^2 \Phi|} \\ D_{\parallel} &\approx \frac{\lambda}{\pi} \frac{1/\sin \Phi}{|\sin^2 \varphi - \sin^2 \Phi|} = \frac{D_{\perp}}{\sin^2 \Phi} \end{aligned} \right\} \quad (41)$$

$$\left. \begin{aligned} Z_{\perp} &\approx \frac{\lambda}{2\pi} \frac{1}{|\sin^2 \varphi - \sin^2 \Phi|} \\ Z_{\parallel} &\approx \frac{\lambda}{2\pi} \frac{1/\sin^2 \Phi}{|\sin^2 \varphi - \sin^2 \Phi|} = \frac{Z_{\perp}}{\sin^2 \Phi} \end{aligned} \right\} \quad (42)$$

These expressions reveal a pronounced dependence on the polarization, namely  $D_{\parallel} > D_{\perp}$  and  $Z_{\parallel} > Z_{\perp}$ , since  $\sin \Phi < 1$ . This dependence was not seen in the original experiment of *Goos* and *Hänchen* [1a] and, therefore, led to several speculations. *Artmann* [15] believed that his theory would predict an incorrect emphasis on polarization, resulting from familiar difficulties with Kirchhoff's boundary conditions. *Von Fragstein* [12] later concluded correctly that the origin of the discrepancy should be traceable to imperfections of the subtle measurements. In a re-investigation *Goos* and (*Lambert*-)*Hänchen* [1b] resolved the discrepancy, and *Wolter* [16] subsequently demonstrated perfect agreement between theory and experiment.

The depth of penetration can be interpreted straightforwardly on the basis of the electromagnetic field in the less-dense medium. This field decays exponentially, namely with the factor  $\exp(2\pi w z/\lambda)$  for E polarization according to (27). At  $e^{-1}$  the absolute value of  $z$  is given by (42a), if (19) is taken into account. *Goos* and *Hänchen* [1a] utilized a similar argument to explain their measurements.

### 3.2 Approximate Description Based on Physical Optics

Historically, *Artmann* [15] first explained the experimental observation of *Goos* and *Hänchen* [1] on theoretical grounds, using physical-optics theories similar to those of *Noether* [8] and *Picht* [7]. He could express the beam displacement in the simple form

$$D_A = \frac{\lambda}{2\pi} \frac{d}{d\varphi} |\delta_r|, \quad (43)$$

where the subscript A refers to "Artmann". The absolute-value notation is employed so that (43) is applicable to either time convention; note the discussion following (19)9. If the phase shift  $\delta_r$  is derived from the Fresnel reflection coefficient of (13a) and (16a), respectively, the beam displacement is given by the Artmann-Wolter expressions

$$D_{AW_{\perp}} = \frac{\lambda}{\pi} \frac{\sin \varphi}{|\sin^2 \varphi - \sin^2 \Phi|} \quad (44a)$$

$$\begin{aligned} D_{AW_{\parallel}} &= \frac{\lambda}{\pi} \frac{\sin \varphi}{|\sin^2 \varphi - \sin^2 \Phi|} \left( \frac{\sin^2 \Phi \cos^2 \Phi}{\sin^4 \Phi \cos^2 \varphi + \sin^2 \varphi - \sin^2 \Phi} \right) \\ &= D_{AW_{\perp}} \left( \frac{1}{\sin^2 \varphi (1 + \csc^2 \Phi)} - 1 \right), \end{aligned} \quad (44b)$$

<sup>9</sup>The reader should bear this reasoning in mind since he will encounter the absolute-value notation in several equations to follow.

where the two subscripts  $\Delta$  and  $W$  refer to "Artmann" and "Wolter". These expressions are valid for angles close to the critical angle for total reflection, but do not hold right at it. Artmann [15] suggested to exclude the narrow angle range of  $(\varphi - \Phi) < 0.3^\circ$ . For angles  $\varphi$  only slightly larger the above equations reduce to the Artmann-v. Fragstein expressions (41).

The expressions so far given for the beam displacement have been evaluated numerically in the range of  $\Delta\varphi = (\varphi - \Phi) < 5^\circ$  for  $\Phi = 10^\circ, 20^\circ, 40^\circ, 60^\circ$  and  $80^\circ$ , respectively. For convenience, all the results are graphically presented in Fig. 7, exhibiting the general description expressed by (34) and (36) in solid curves. The numerical results obtained from (44) are indicated by the strings of open dots. They agree very closely with the general description, except at a large  $\Phi$  value. This deviation is not entirely surprising since (44) suffers from the shortcoming of predicting a nonvanishing beam displacement in the limit of grazing incidence, as pointed out in Reference 13. The Artmann-v. Fragstein expressions (41) are illustrated by the strings of dots. We notice at once the poor agreement in the case of H polarization at small  $\Phi$  values. For E polarization the numerical results deviate by a few percent. However, since the magnitude of the beam displacement is so small, these deviations are hardly noticeable in Fig. 7; the dots lie within the little circles. As  $\Phi$  increases, the deviation decreases rapidly and the simple Artmann-v. Fragstein expressions describe rather well the beam displacement at medium  $\Phi$  values. It should be noted that this range contains the important case of total reflection at the glass/air interface.

Wolter [16] investigated the Goos-Hänchen effect on the basis of the minimum-ray definition developed by himself [21]. He considered the simultaneous reflection of two out-of-phase plane waves propagating under the small angle  $\Delta$  and intersecting the interface at the angle  $\varphi$  and  $\varphi' = \varphi - \Delta$ , respectively. The reflected minimum ray is then displaced parallelly by

$$D_W = \frac{\lambda R - R' \Delta}{i\pi R + R' \Delta}, \quad (45)$$

where the subscript  $W$  refers to "Wolter", and the Fresnel reflection coefficients  $R$  and  $R'$  are given by either (13a) or (16a) for the corresponding angle  $\varphi$  or  $\varphi'$ . The above expression is complex; its real part represents the beam displacement and its imaginary part is a measure for the "blurring" of the minimum. At  $\text{Im}\{D_W\}$  the intensity increases to twice its value at the minimum; and thus  $2\text{Im}\{D_W\}$  may be interpreted as the width of the reflected minimum ray.

Wolter pointed out that in the limit as  $\Delta \rightarrow 0$  the above expression can be reduced to

$$\begin{aligned} D_W &\simeq \frac{\lambda}{2\pi i} \frac{1}{R} \frac{dR}{d\varphi} \\ &= \frac{\lambda}{2\pi} \frac{d}{d\varphi} |\text{arc}R| - i \frac{\lambda}{2\pi} \frac{1}{|R|} \frac{d}{d\varphi} |R|. \end{aligned} \quad (46)$$

This equation may be looked at as a simple, but significant extension of (43). At ideal total reflection  $|R| \equiv 1$  and, since  $\text{arc}R$  is given by the phase angle  $\delta_r$ , (46) reduces to (43). Therefore, the equations (44) are termed the Artmann-Wolter expressions.

Equation (46) reveals a number of important facts in light of the aforementioned interpretation of (45). If we assume for the moment that the two interfacing media are ideally lossless, then at total reflection  $|R| \equiv 1$  and the totally reflected minimum ray is strictly displaced, whereas at partial reflection ( $\varphi < \Phi$ )  $\text{arc}R \equiv 0$  and the partially reflected minimum ray is only blurred. In general, the minimum ray is both displaced and blurred, depending upon the angle of incidence and the properties of the interfacing media.

In Wolter's theory [16] the index of refraction may be complex, thus providing the possibility of accounting for absorption in the dielectrics as well as for metallic media. A comprehensive treatment of this topic is deferred to Chapter 6. Only the results for reflection at a silvered surface, pertaining to the present subject, are reproduced here. Assuming  $\sqrt{\epsilon_1} = 1.52$  and  $\sqrt{\epsilon_2} = n_2 - ik_2$  with  $n_2 = 0.18$  and  $k_2 = 3.31$  for silver at  $\lambda_0 = 5500 \text{ \AA}$ , Wolter obtained for the beam displacements  $D_{W_I} = 0.12\lambda$  and  $D_{W_{II}} = -0.18\lambda$  at  $\varphi = 45^\circ$ . Attention is directed to the significant fact that, depending upon the polarization, the beam appears to be reflected by a virtual surface located either below or above the interface. In each case the "depth of penetration" amounts to only a few percent of the already small beam displacement. Those results have a bearing upon the interpretation of the measurements since the reference beam has been reflected metallically at a silvered strip, as indicated in Fig. 2. — It seems worth mentioning that replacing the real quantities  $n$  and  $w$  of the Artmann-v. Fragstein expressions (41) and (42) by complex quantities in the sense of metal optics leads to results approximately equal to those of Wolter [46]. This observation is not unexpected since the Artmann-v. Fragstein expressions are contained in the Artmann-Wolter expressions as first-order approximations. In our theory a complex dielectric constant would lead to some difficulty in treating  $A(\beta_g)$  so elementary, as outlined in connection with (23).

Goos and Hänchen [1a] first succeeded in measuring the beam displacement in a novel experiment discussed in connection with Fig. 2. They clearly demonstrated the dependence on the angle of incidence, but could not find initially a dependence on the polarization. The latter observation was rather puzzling from the theoretical point of view and led to speculation, as indicated in Section 3.1. Goos and Hänchen [1b] later resolved the issue by measuring the theoretically predicted polarization dependence in a refined experiment. All questions were finally settled by Wolter [16] who demonstrated excellent agreement between theory and experiment, as shown in Fig. 8. Wolter recognized that to measure such a subtle effect requires the application of his minimum-ray definition [21]. This ingenious method provides a 16-fold improved resolution over the Goos and Hänchen technique, as indicated in Fig. 8. The measured and calculated data presented in this figure are normalized to the vacuum wavelength  $\lambda_0$  rather than to  $\lambda = n\lambda_0$ , as done throughout this

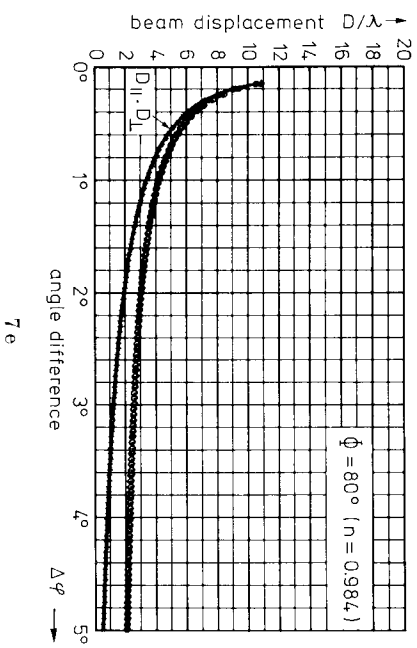
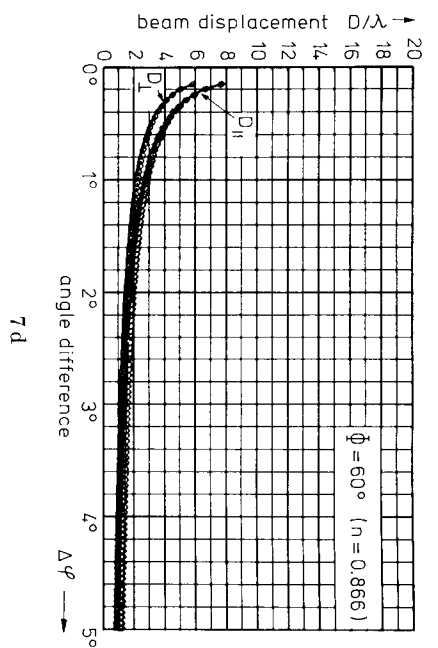
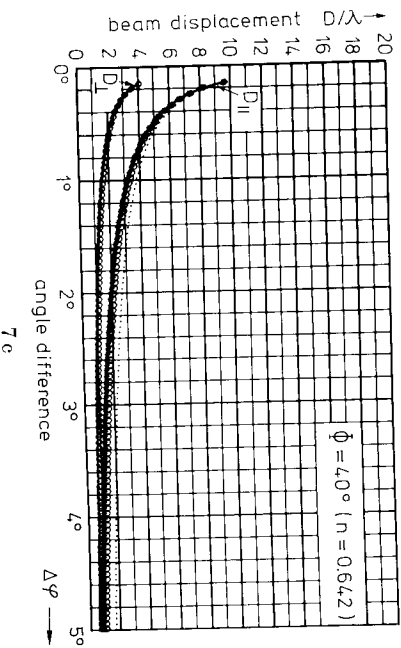
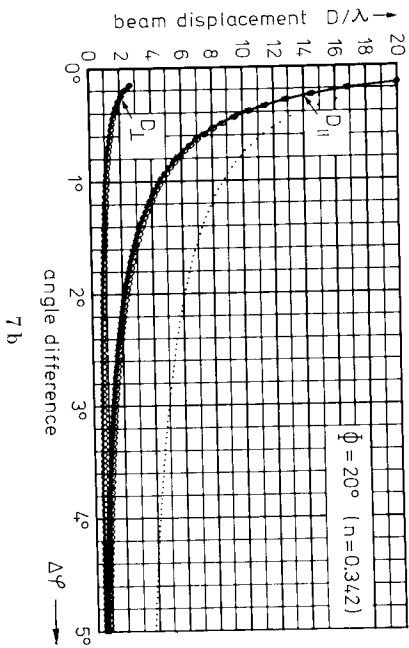
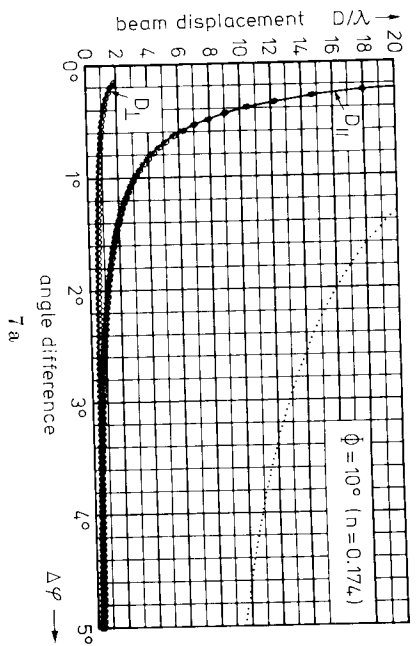


Fig. 7. The beam displacement  $D$  versus angle difference  $\Delta\varphi = (\varphi - \phi)$  is displayed assuming a critical angle for total reflection  $\phi$  of either  $10^\circ$  (a),  $20^\circ$  (b),  $40^\circ$  (c),  $60^\circ$  (d) or  $80^\circ$  (e). The solid curves represent the general descriptions given by either (34) or (36), the strings of open dots illustrate the expressions (44) derived by *Artemann* and *Wolter*, and the string of dots depicts the approximation (41) suggested by *Artemann* and *v. Fragstein*. [Note that the dots representing (41a) for  $\perp$  polarization lie within the circles for the corresponding equation (44a).]

paper. For total reflection at the glass/air interface investigated by *Wolter* we have  $\lambda = \lambda_0/1.52$  since  $n = 1/1.52$ . The small correction due to the reflection of the reference beam at the silvered strip, mentioned above, has been taken into account in preparing Fig. 8. *Wolter*, after a detailed consideration of possible errors in the measurement, concluded that the measured points for  $D/\lambda_0$  are, on the average, accurate at least to 0.3; in narrower angle ranges the error was found to be as small as 0.05 to 0.1.

The curves shown in Fig. 8 were, strictly speaking, calculated on the basis of *Wöller's* extended theory to be discussed below. The Artmann-Wölder expressions (44) are only valid for  $(\varphi - \Phi) > 0.3^\circ$ . In this range the approximate ( $\Delta \rightarrow 0$ ) and extended ( $\Delta = 2.5 \times 10^{-3}$ ) theories of *Wöller* yield, for all practical purposes, identical displacements, as may be inferred from Fig. 9. The theoretical results so far presented are, therefore, completely substantiated by measurement. This leads one to conclude that the Artmann-Wölder expressions (44) are not only simpler than our general formulas (34) and (36) but also accurate enough for most applications. Their shortcoming in the limit of grazing incidence is not severe because the *Goos-Hänchen* effect is significant only in the neighborhood of the critical angle for total reflection and negligible everywhere else.

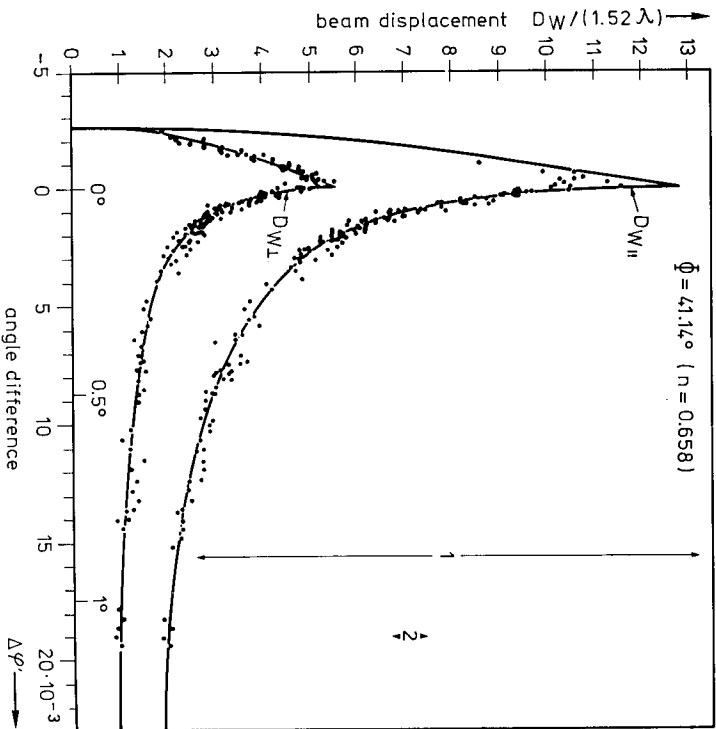


Fig. 8. The beam displacement  $D_w$  versus angle difference  $\Delta\varphi' = (\varphi - \Phi)$  in degrees and radians is presented for both polarizations. [16]. The wavelength  $\lambda$  is measured in the optically denser medium. The measured and calculated ( $\Delta = 2.5 \times 10^{-3}$ ) results demonstrate the excellent agreement between theory and experiment.  $\leftarrow 1 \rightarrow$  indicates the minimum beam widths in the measurements reported by *Goos* and *Hänchen* [1], whereas  $\leftarrow 2 \rightarrow$  shows the width of the minimum ray in *Wöller's* experiment. (Reproduction through the courtesy of H. *Wöller*, University of Marburg, Germany).

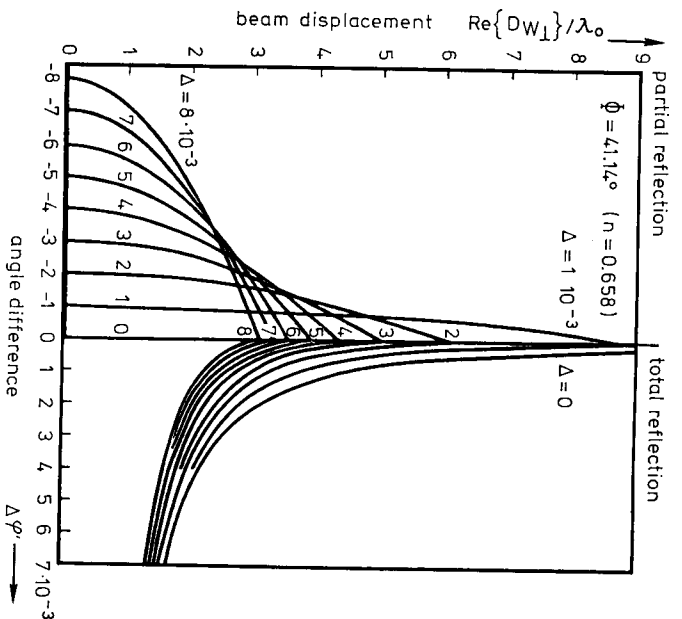


Fig. 9. The beam displacement  $D_{wI}$  in vacuum wavelength  $\lambda_0$  versus angle difference  $\Delta\varphi' = (\varphi' - \Phi)$  in radians is depicted in the immediate vicinity about the critical angle for total reflection  $\Phi$ , assuming different values for  $\Delta$ . [16]. (Reproduction through the courtesy of H. *Wöller*, University of Marburg, Germany).

### 3.3 Description of Transition Region from Total to Partial Reflection

The description of the *Goos-Hänchen* effect so far presented does not hold in the immediate neighborhood of the critical angle for total reflection, as stated above. In this section the transition from total reflection to partial reflection, including the previously excluded angle range of  $(\varphi - \Phi) < 0.3^\circ$ , is considered on the basis of *Wöller's* extended theory [16]. Substituting the corresponding Fresnel reflection coefficients into *Wöller's* expression (45) yields after a straightforward calculation

$$D_{w\perp} = \frac{\lambda}{\pi \Delta} \frac{1}{n} \left\{ \cos\varphi' \cos[\arcsin(\sin\varphi/n)] - \cos\varphi \cos[\arcsin(\sin\varphi'/n)] \right\} \quad (47a)$$

and

$$D_{w\parallel} = \frac{\lambda}{\pi \Delta} \frac{1}{n^2} \frac{1}{n} \left\{ \cos\varphi' \cos[\arcsin(\sin\varphi/n)] - \cos\varphi \cos[\arcsin(\sin\varphi'/n)] \right\} \quad (47b)$$

where  $\varphi$  and  $\varphi'$  denote the angles of incidence of the two out-of-phase plane waves propagating under the small angle  $\Delta = \varphi - \varphi'$ .

If *Wolter* [16] numerically evaluated (47) for several values of  $\Delta$ ; his results are reproduced in Fig. 9 through 11. Fig. 9 illustrates the real part of (47a), representing the beam displacement, versus the angle difference  $\Delta\varphi' = \varphi' - \Phi$ , where  $\varphi'$  designates the wave with the steeper angle of incidence. We note the familiar functional dependence in the range of  $\Delta\varphi' > 0$ . For  $\Delta\varphi' < 0$  the beam displacement decreases rapidly depending upon the value of  $\Delta$  and becomes zero at  $\Delta\varphi' = -\Delta$ . That is to say, (47) may be interpreted as representing the resultant beam displacement of two plane-wave components.

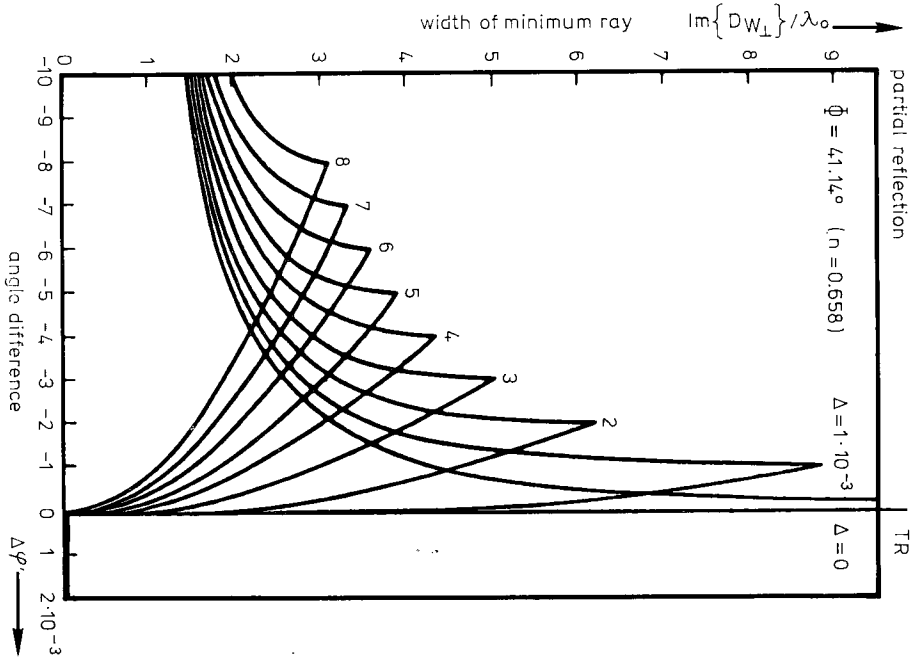


Fig. 10. The width of the minimum ray in vacuum wavelength  $\lambda_0$  versus angle difference  $\Delta\varphi' = (\varphi' - \Phi)$  in radians is depicted in the immediate vicinity about the critical angle for total reflection  $\Phi$ , assuming different values for  $\Delta$ , [16]. (Reproduction through the courtesy of H. Wolter, University of Marburg, Germany.)

When the component with the steeper incidence crosses over to the region of partial reflection, its displacement becomes identically zero, in a sense leaving behind the displacement of the second, slightly less steep component. Finally at  $\Delta\varphi' = -\Delta$  both components have crossed over to the region of partial reflection. - Fig. 10 depicts the width of the minimum ray versus the angle difference  $\Delta\varphi'$ . This width is obviously zero as long as both plane-wave components are confined to total reflection. At  $\Delta\varphi' = 0$ , where the more steeply impinging component crosses over to the region of partial reflection, the minimum ray is blurred discontinuously. As  $\Delta\varphi'$  decreases further and exceeds  $-\Delta$ , the width of the minimum ray settles down to some finite value. - The dependence of the beam displacement on the polarization of the incident waves is demonstrated in Fig. 11. The dependence decreases as  $\Delta\varphi'$

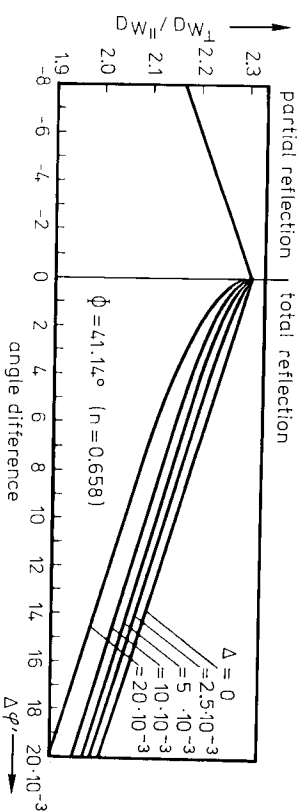


Fig. 11. The polarization ratio ( $D_{w_{\parallel}}/D_{w_{\perp}}$ ) versus angle difference  $\Delta\varphi' = (\varphi' - \Phi)$  in radians is depicted in the immediate vicinity about the critical angle for total reflection  $\Phi$ , assuming different values for  $\Delta$ , [16]. (Reproduction through the courtesy of H. Wolter, University of Marburg, Germany.)

decreases to zero and is absent in the range of negative  $\Delta\varphi'$ . - As noted in connection with (46), the foregoing discussion applies to the ideal case of nonabsorbing media. Assuming a complex index of refraction to account for absorption will not alter our discussion in any essential point; it will merely introduce smooth transitions in place of the abrupt transitions as the angle difference  $\Delta\varphi'$  is varied.

As pointed out in Section 3.2, *Wolter* [16] substantiated his calculations by experiment; the results are reproduced in Fig. 8. We note full agreement between theory and experiment for both polarizations in the entire angle range of interest. This excellent agreement cannot be stressed enough in view of the subtle experiment which had to be performed.

*Armann* [44] also investigated the transition region from total to partial reflection, thus supplementing his classical treatment of the *Goos-Hänchen* effect with the narrow angle range of  $(\varphi - \Phi) < 0.3^\circ$ , previously excluded [15]. He recognized the similarity between his treatment and *Sommerfeld's* rigorous solution of the diffraction problem on an infinitesimally thin, perfectly conducting half-plane [47]. Taking advantage of this similarity,

*Armann* related the transmitted beam at the onset of partial reflection to v. Schmidt's lateral wave, to be treated in Section 5.2. — The lateral wave was introduced by v. Schmidt [25] to describe the "traveling reflection", indicated in the Introduction. — He then showed that the N-times totally reflected beam in the experiment of *Goos* and *Hänchen* [1] can be interpreted in terms of that transmitted beam at a particular plane. *Armann* found that in the immediate neighborhood of the critical angle, the center of the totally reflected beam is not only shifted along the interface by the amount [44]

$$\bar{X} = \frac{\lambda}{2\pi} \frac{2Np}{\sqrt{2 \sin^2 \Phi} \cdot \tan \Phi} \sqrt{\varphi - \Phi} \quad \text{with} \quad (\varphi - \Phi) \approx \frac{1}{N^2} \quad (48a)$$

where  $p$  is the polarization factor, but also distorted in its intensity distribution. This distortion is essentially independent of the intensity distribution of the incident beam. On account of v. Schmidt's lateral wave, the beam displacement at the critical angle is not infinite, but assumes the finite value, [44]

$$\bar{X} |_{\varphi = \Phi} = \frac{\lambda}{2\pi} \frac{9N^2 p^2 \cos \Phi}{\sin^2 \Phi} \quad (48b)$$

We note that the quasi-displacement (48a) is proportional to  $Np$ , whereas its limiting value (48b) is proportional to  $(Np)^2$ . Explicitly the polarization factor  $p$  is 1 for E polarization and  $1/\sin^2 \Phi$  for H polarization. (*To be continued*)

## Über den Maximalwert des photometrischen Strahlungäquivalentes

Von J. Krockmann

Institut für Lichttechnik der Technischen Universität Berlin

Eingegangen am 22. Mai 1970

### Inhalt

Durch die internationale Temperaturskala 1968 sind die Zahlenwerte für die Konstanten  $c_1$  und  $c_2$  des Planckschen Strahlungsgesetzes und die platin-Erstarungstemperatur  $T_{pl}$  neu festgesetzt. Dadurch ändern sich auch die Maximalwerte des photometrischen Strahlungäquivalentes  $K_m$  für Tagesehen und  $K'_m$  für Nachtsehen. Die neuen Werte ergeben sich zu  $K_m = 673 \text{ lm/W}$  und  $K'_m = 1725 \text{ lm/W}$ . Der Verlauf des Maximalwertes des photometrischen Strahlungäquivalentes  $K^*_m$  im mesopischen Bereich wird behandelt.

### Abstract

**The Maximum Luminous Efficiency.** The values of the constants  $c_1$  and  $c_2$  of Planck's law and the temperature of the Platin-melting point are fixed by the International Temperature Scale 1968. By this the photopic and scotopic maximum luminous efficiency is changed. The new values are:  $K = 673 \text{ lm/W}$  and  $K'_m = 1725 \text{ lm/W}$ . Values of the maximum luminous efficiency within the mesopic range are given too.

### 1. Begriffe

Die lichttechnischen Größen ergeben sich für Tages- bzw. Nachtsehen aus den entsprechenden strahlungsphysikalischen Größen zu [1]:

$$X_V = K_m \int_{380 \text{ nm}}^{780 \text{ nm}} X_{ex} V(\lambda) d\lambda \quad (1)$$

$$X'_V = K'_m \int_{380 \text{ nm}}^{780 \text{ nm}} X_{ex} V'(\lambda) d\lambda \quad (2)$$

$X_V$  die lichttechnische Größe für Tagesehen, z. B. die Leuchtdichte  $L_V$ ,  
 $X'_V$  die lichttechnische Größe für Nachtsehen, z. B. die skotopische Leuchtdichte  $L'_V$ ,